Observing the dynamics of waterborne pathogens for assessing the level of contamination

Isabella McKenna, Francesco Tonolini, Rachael Tobin, Jeremie Houssineau, Helen Bridle, Craig McDougall, Isabel Schlangen, John S. McGrath, Melanie Jimenez and Daniel E. Clark

***Abstract*—In environments of scarce hygiene it is of primary importance to detect potentially harmful concentrations of pathogens in drinking water. In many situations, however, accurate analysis of water samples is prohibitively complex and often requires highly specialised apparatuses and technicians. In order to overcome these limitations, a method to employ video processing to assist microfluidics water filtering apparatuses is proposed. Through the automated analysis of videos captured at the output of such devices it is possible to extract useful information that could control an autonomous calibration, hence eliminating the need of an expert and possibly leading to the construction of readily employable water quality assessing devices.**

***Index Terms*—Waterborne pathogens, microfluidics, tracking, water contamination, detection, classification.**

INTRODUCTION

Often during major combat situations hygiene can be poor and access to potable water limited. Additionally, military personnel can also be exposed to potentially contaminated water during other scenarios, e.g., training and relaxation or deployment for humanitarian aid. Illness evidently reduces operational capability and is highly undesirable. During the 1990s norovirus outbreaks on US aircraft carriers affected up to 44% of the crews [1]. Other waterborne pathogens, e.g., protozoa such as *Cryptosporidium* and *Giardia* [2], [3], [4], are also potential risk factors though much less is known about their prevalence in military disease outbreaks. However, these pathogens are resistant to disinfection by chlorine and have extremely low infectious doses explaining why these have been responsible for major outbreaks of waterborne gastroenteritis in Europe and the US [5].

Water quality monitoring methods [6], [7], [8], especially those which are automated and easy to use, could play a significant role in reducing the risk of disease in military scenarios. Water utilities regularly monitor water quality to ensure the safety of supply. However, existing methods are time consuming and require highly trained microbiologists [9].

In this article new approaches to water monitoring, focussing on the use of automated microfluidic systems are being developed. Microfluidics is an emerging area of focus for waterborne pathogen sample processing and detection [10].

Within microfluidics devices observing the position and flow behaviour of pathogens is critical to the optimisation of designs and operating parameters as well as in the development of early warning approaches where the presence of a particle of a particular size or shape at a certain channel location could indicate a pathogen.

The method of pathogen observation proposed hereafter exploits video processing techniques to first detect and then classify particles in the output flow of a microfluidics apparatus. A digital camera positioned at the outlet of the device records the flow of particles. In the detection stage, the video frames are individually processed to retrieve position coordinates and size estimation. The obtained data is then fed into a Hypothesised filter for Independent Stochastic Populations (HISP) [11] which returns particle tracks and velocity information and which is able to classify particles according to their dynamic behaviour.

I. MICROFLUIDICS DEVICES

To properly assess the level of water contamination, an efficient detection system should be able to screen out other particles present in the water, evaluate the concentration of pathogens in the water sample and give the means to determine species and viability of the organisms.

Retrieving and correctly interpreting the output of such devices could make the engineering of automated calibration schemes possible. Miniaturised fluidic devices in which the output can be directly observed and recorded with a camera are optimally suited to achieve automation. Given their means of particle segregation and the ease of recording the output flow with a digital camera, we identify two suitable set-ups. Passive hydrodynamic focussing, which exploits the geometries of microchannels to sort particles, and dielectrophoresis devices, in which an applied electric field segregates the particles of interest by viability and/or species, thus indicating infectivity. Preliminary results have been obtained for these two set-ups for particles as small as bacteria.

A. Passive hydrodynamics

As part of the Aquavalens project, Jimenez et al. have developed a sample processing microfluidics device based on a passive hydrodynamic method[1]. By controlling the flow rate in a carefully designed channel, chosen particles can be focused along certain streams within the channel, see Figure 1. Viable and non-viable pathogens and different species of pathogens usually show dissimilarities in size and deformability, which determines their behaviour and final lateral channel position. Therefore, they can be collected into different outlets as required.

Detection methods applied to the output streams of the device could determine the effectiveness of the approach and

[1]further design details cannot be given due to a pending patent application.

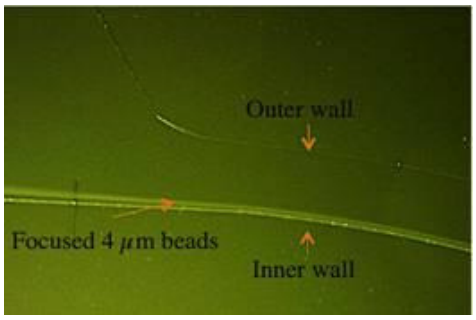

Fig. 1. Image of the device working with a high concentration of beads of a particular size. The image illustrates how particles of a particular size are sorted into a narrow size band, relative to the width of the channel, and can therefore be concentrated and collected by appropriate design of the outlet area. Different size particles will be located at different points across the channel.

produce a quantitative analysis of the outlet flows. These detections could also act as an early warning system for pathogen presence.

B. Dielectrophoresis

Polarisable particles such as biological cells can be trapped and manipulated by applying an inhomogeneous electric field in a phenomenon called dieloctrophoresis (DEP) [5].

The direction and magnitude of the force acting on the particles depend on the polarisability of the particles with respect to the medium. Viable and non-viable pathogen oocysts have been shown to behave differently under the force of the same electric field [12].

Figure 2 shows the output of a DEP electrorotation device. A set of carefully positioned electrodes creates a pattern of electric fields to trap particles in the centre of the device and allow them to rotate. In the case of pathogen filtering, it has been shown that organisms behave differently according to their viability. In particular, their rate and direction of rotation differ; non-viable oocysts tend to rotate clockwise and faster than viable ones.

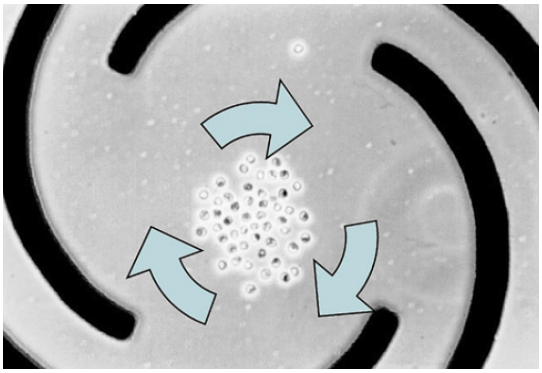

Fig. 2. Image of the output of a DEP electrorotation device. The electrodes (in black) generate an electric field such that the particles are kept in a specific area, but can rotate within it [12].

A continuous flow system has recently been developed utilising DEP to direct oocysts to different outlets, see Figure 3.

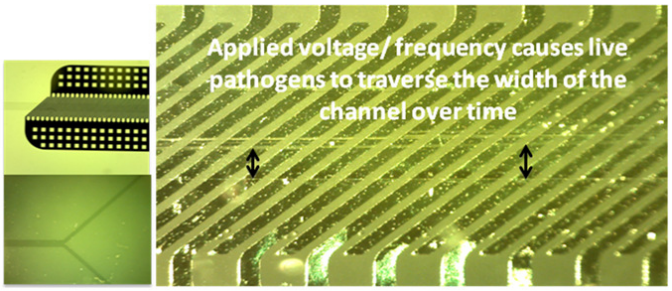

Fig. 3. The images on the left indicate the device design. Top picture shows the central channel where electrodes are located. The bottom picture shows the outlets where particles influence by the DEP have moved to the top half of the channel and are collected through the top outlet. The right image shows two different particle trajectories indicating how the degree of separation between then increases along the channel..

Video processing techniques can be applied to characterise the performance at different flow rates and electric fields, in order to assist in determining optimal operating parameters.

II. Analysis

The aim of an automated video analysis in this context is that of extracting meaningful information associated with each of the observed particles individually, such as their position, size and velocity, as time evolves. The obtained data can then be made use of in constructing indicators of statistical behaviour that are descriptive of the system and readily provide useful knowledge for contamination level assessment or apparatus calibration response.

To perform such information extraction, the procedure consists of two main steps; a detection step, which retrieves position coordinates and related uncertainty and estimated size for each particle at each video frame, and a classification step, which exploits a multi-object filter to obtain tracks of the detected objects and classify them according to their appearance or behaviour.

A. Detection

To perform tracking of objects in microfluidics videos it is necessary to first obtain accurate detections of such objects for each video frame. In other words, it is necessary to extrapolate an estimate of the position and associated uncertainty for each object in every frame. An important condition on the retrieved information is that the positions and deviations obtained from the video frames are independent from one another. This is because the tracker relies on the assumption that observations at different time steps are not correlated with each other.

The problem is to recognise objects of interest in an image according to the known features that make them distinguishable from the rest of the image. The objects that are processed through different microfluidics set-ups can be of varied nature and generally the features that make them recognisable have to be chosen depending on the specific situation [13], [5].

In most biological applications of microfluidics particle sorting, however, the particles of interest tend to present a roughly spherical shape and it is precisely this feature, along

with their intensity difference with the immediate surrounding, that was largely exploited in the hereafter described detection method.

Prior to any recognition algorithm, a binary image is generated from the video frame under analysis via thresholding. This operation needs to be applied either to the image or to its negative, depending whether the particles to be detected are darker or brighter than the background.

To seek for circles in the binary image, with conditions imposed on the possible radii, the first part of the algorithm employed uses the circular Hough transform. Such method takes all pixels of high intensity gradient as candidate perimeter pixels p_i. Each candidate pixel is then made to cast a vote on the pixels that trace out a circular perimeter of different potential radii r_g around it and if a particular combination of pixel location and guess radius has a vote over a certain threshold that pixel location and guess radius determine a detected circle [14], [15]. That is, given an image $I \in \mathbb{R}^{n\times m}$, a votes array $V_g \in \mathbb{R}^{n\times m}$ for each guess radius r_g is computed as follows

$$V_g = \sum_{i=1}^{k} C(p_i, r_g), \tag{1}$$

where $C(p_i, r_g) \in \mathbb{R}^{n\times m}$ is an array of ones on the perimeter of a circle with center p_i and radius r_g and zeros everywhere else. k is the number of perimeter candidate pixels. In every vote array V_g, those elements that are over a certain threshold determine a detected circle in the image I with the coordinates of such an element as its center and r_g as its radius.

It is worth noting that this first step provides not only the position of the detected objects, but also their radius and hence their surface area. It is therefore possible to classify particles according to their size and group them in categories that have approximately the same mean area.

The above described method proved to be quite successful at recognising and locating single particles with limited flow rate. However, in microfluidics channels, particles occasionally move at faster rates or agglomerate in small clusters.

To address such situations, the second step in the detection algorithm considers all objects within a given area interval as candidate high speed objects or agglomerates. Their surface area is then compared with the mean area of each of the previously detected spheres groups. Objects which are found to have an area equal to that of a particular category within a certain tolerance are classified as belonging to that category. Objects which are found to be significantly smaller than any of the previously observed sizes are discarded as unimportant features in the image. Objects which are found to have an area significantly bigger than the area of any of the categories are labelled as agglomerates.

To locate objects within an estimated agglomerate, a small subsection of the image containing the agglomerate is convolved with different circles, each having the mean size of a particular category. The position and radius that yields the highest value in the convolved image are taken as center and radius of a detected object. The detected object is then subtracted from the image and the process is repeated until the remaining agglomerate has an area which is considerably less than that of any category.

B. Classification

Tracking and classification are performed jointly in order to provide a full probabilistic picture of the situation. This has been made possible with the introduction of a tracking framework modelling partially distinguishable populations [11]. This level of generality is required to perform principled multi-object estimation where specific information about objects, referred to as track, is propagated. This, in turn, allows for performing classification by distinguishing objects with different behaviours. The multi-object estimation algorithm that is used in this article is called the Hypothesised filter for Independent Stochastic Populations, or HISP filter [11], [16], [17], and is an approximated but tractable version of a multi-object Bayes filter. Joint tracking and classification has already been performed with the HISP filter for different applications such as harbour surveillance [18]. The principle of the approach is to perform multi-object estimation on a population that is composed of two or more sub-populations. In order to obtain information on this additional aspect, each sub-population should have distinct characteristics such as different motion models or different trajectories. In this article, we consider both location- and motion-based classification.

This way of classifying particles do not rely on visual features that could be obtained from the video. In consequence, the quality of the images acquired by the digital camera does not affect the performance of the classification algorithm as long as the detection technique described in Section II-A can be applied.

III. Experiment

In order to demonstrate the proposed detection algorithm in a controlled environment, it was necessary to simulate a flow of particles in a microfluidic channel in vitro.

This was achieved by using spherical beads of diameters 7 microns and 10 microns suspended in a mixture of water and liquid detergent in a flow channel 300 microns in diameter. Adjustable flow paths were set up prior to the particles entering the channel using an acoustical sorting process which created resonant conditions using an ultrasonic transducer and a reflective boundary.

The standing wave that arose due to these resonant conditions created nodes which behave as pressure maxima and minima with axial forces drawing particles towards them; the particles were then drawn together by lateral forces and particle-particle interactions, resulting in precise flow streams.

The particles then entered the channel until displaced approximately 150 microns orthogonal to the direction of travel through laser controlled optical tweezing. The beam power and waist were chosen for optimal performance based on the desired particle size and density.

The video was captured with a Prosilica EC1280 firewire camera imaging the outlet of the above described apparatus

and was shot at 23 frames per second; a captured frame can be viewed in Figure 4.

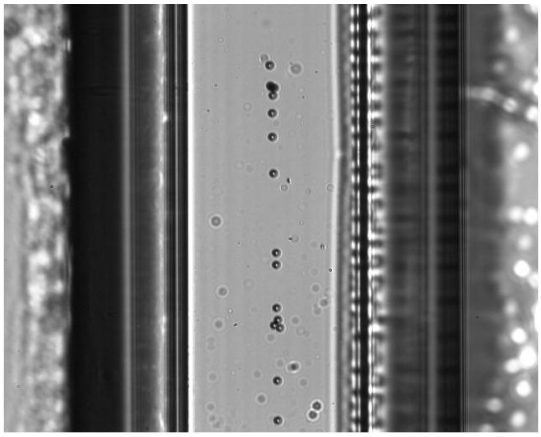

Fig. 4. Image of the output of a DEP electrorotation device. The electrodes (in black) generates an electric field such that the particles are kept in a specific area, but can rotate within it.

A. Detection

The detection method was found to be very effective provided the particles to be detected do not differ by more than a factor of two in radius from each other and that the speed at which they move is still sufficiently low such that the particle does not move by more than twice its size in the acquisition time of one frame. These assumption may not always hold for every particle sorting apparatus and the method might need to be modified to accommodate certain situations. In the particle sorting data that were processed and are reported here, however, these assumption mostly held true and the detection was found to be quite accurate. Results of the detection method described above are shown for one particular frame taken from a sorting microfluidics video in Figure 5, where the particles detected by the first part and the second part of the algorithm are highlighted in different colours.

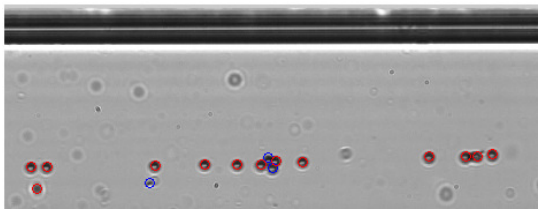

Fig. 5. Detected locations of particles overlaid on the video frame they have been extracted from. The detections highlighted in red are obtained as a result of the circular Hough transform filtering and the detections highlighted in blue are obtained employing the second section of the algorithm. It can be seen how, although the circular Hough transform is successful at recognising most of the particles, it misses particles which are part of a cluster and a particle that moves faster than the others. The second section of the algorithm effectively compensates for such missed detections.

As for the deviations associated with the retrieved positions, these were taken to be symmetric and the ones related to particles detected through the first step were set to roughly their retrieved diameter and those obtained from the second step were set to twice their diameter. This is because successful detection through the circular Hough transform resulted to be very precise in this context, whereas detection of fast moving particles and clustered particles yields less precise estimates of their centre positions.

In order to assess the proposed detection method, the performance of the algorithm in terms of cardinality and localisation has been evaluated using the OSPA distance [19] on simulated data. For the simulation to be sufficiently representative of the real problem, an average number of 12 synthetic beads of different sizes have been added to a real background in 40 different configurations including agglomerates. The average OSPA distance, with a 2-norm and a cut-off of $10\,\mathrm{px}$, is found to be equal to 0.64 with a standard deviation of 0.0818. This result indicates that most of the beads are found in the image without creating many false positives and that these beads are accurately localised.

B. Classification

We consider the experiment described in Section III and perform the classification with the following parameters: sorted and unsorted beads both have a motion model based on a constant velocity up to the position of the laser. The unsorted beads are unaffected by the laser whereas the sorted ones are diverted by it, which is modelled as a force applied orthogonally. In the latter model, two additional forces are considered: the first one is the friction due to the viscosity of the fluid and the second one is a trapping effect due to the laser, which compensates for the motion of the fluid along the channel. The uncertainty on each motion model is characterised by an additive noise on the acceleration. A location-based classification is utilised for counting the number of beads that exit the field of view of the camera through the far end of the channel and the number of beads that are stopped on the border of the channel around the location of the laser. The obtained numbers are indicated in the titles of Figures 6(a) and 6(b). Two examples are given in these figures where tracks corresponding to beads with different behaviours are displayed with various colours. To handle the fact that all beads have the same motion model up to the position of the laser, an additional class named "Unclassified" is created and associated to beads for which the classification is too uncertain. Specifically, the probability for one bead to be part of a given class has to be above 75% for the corresponding track to be displayed with the associated colour.

IV. Conclusion

The employment of video processing techniques to assist the operation of microfluidic devices could allow for the production of portable, readily employable and extremely accurate water contamination assessing tools, ideally suited for the needs of military operations. The detection method presented here allowed efficient detection of differently sized microspheres flowing through the outlet of a microfluidic device. The two techniques described in section II-A proved to be

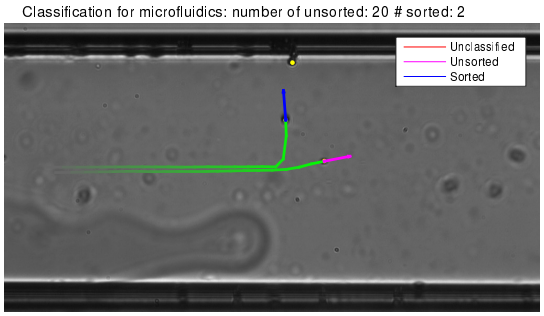

(a) Time step 606: one bead is being diverted by the laser (blue) while the other one has not been affected (magenta)

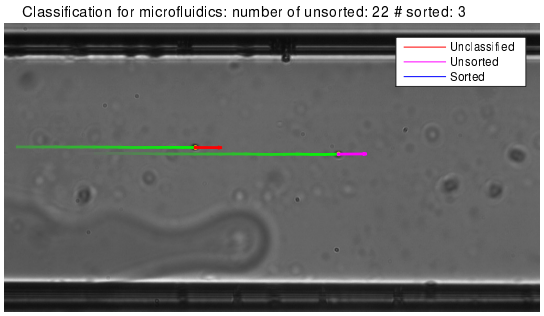

(b) Time step 673: one bead is not classified yet (red) and the other one has not been affected by the laser (magenta)

Fig. 6. Examples of classification with the HISP filter. Observations are indicated in yellow, tracks are displayed with different colours depending on their classification, and the trajectory for each track is shown in fading green.

effective at obtaining accurate estimates of particle positions and sizes in every video frame with tolerable amounts of false alarms and missed detections.

The classification of the observed particles was carried out employing the HISP filter. Such algorithm was able to extract particle tracks and associated velocity along with the related uncertainties. The obtained information was then used to classify the objects into sorted and unsorted particles. Having such detailed information for every single particle flowing through the outlet of a microfluidic channel gives a complete measure of the apparatus state of operation and hence can be used as a reliable and automated feedback for the calibration of the device through the optimisation of its many parameters.

As in most cases the relationship between output particle behaviour and system parameters is known, the data retrieved by the classification can be used to control a proper automated response. For instance, if a stream of particles appears clustered and poorly focused at the outlet of a spiral channel device, it can be deduced that the flow rate through the channel is too low. From the autonomously obtained data it is then possible to quantify these characteristics of the stream and trigger an appropriate increase of flow rate. In many cases pathogen size and dynamic behaviour are also indicators of species and viability, hence a measure of the level of contamination of the sample can be deduced from a classification method analogous to that described above.

ACKNOWLEDGMENTS

Helen Bridle, John McGrath and Melanie Jimenez are supported by STFC, the EU Aquavalens project and Scottish Water. Jeremie Houssineau and Daniel E. Clark are supported by DSTL Task ED TIN 2-3. Isabel Schlangen has a PhD scolarship from the Edinburgh Super-resolution Imaging Consortium (ESRIC). Craig McDougall is supported by the EPSRC as a post doctoral researcher. Daniel Clark is supported by the EPSRC/Dstl University Defence Research Centre on Signal Processing (UDRC) Phase 2 (EP/K014227/1).

REFERENCES

[1] J. J. Wijnker and H. de Man, "Assessing the waterborne risk of a norovirus infection for military personnel in the netherlands," *Nederlands militair geneeskundig tijdschrift*, vol. 67, no. 1, pp. 16–18, 2014.

[2] M. Smith and K. C. Thompson, *Cryptosporidium: the analytical challenge*. Royal Society of Chemistry, 2001, vol. 1.

[3] F. Chen, K. Huang, S. Qin, Y. Zhao, and C. Pan, "Comparison of viability and infectivity of cryptosporidium parvum oocysts stored in potassium dichromate solution and chlorinated tap water," *Veterinary parasitology*, vol. 150, no. 1, pp. 13–17, 2007.

[4] C. C. Tam, L. C. Rodrigues, L. Viviani, J. P. Dodds, M. R. Evans, P. R. Hunter, J. J. Gray, L. H. Letley, G. Rait, D. S. Tompkins *et al.*, "Longitudinal study of infectious intestinal disease in the uk (iid2 study): incidence in the community and presenting to general practice," *Gut*, vol. 61, no. 1, pp. 69–77, 2012.

[5] H. Bridle, M. Kersaudy-Kerhoas, B. Miller, D. Gavriilidou, F. Katzer, E. A. Innes, and M. P. Y. Desmulliez, "Detection of cryptosporidium in miniaturised fluidic devices," *Water research*, vol. 46, no. 6, pp. 1641–1661, 2012.

[6] T. M. Straub and D. P. Chandler, "Towards a unified system for detecting waterborne pathogens," *Journal of Microbiological Methods*, vol. 53, no. 2, pp. 185–197, 2003.

[7] P. T. Monis, S. Giglio, A. R. Keegan, and R. A. Thompson, "Emerging technologies for the detection and genetic characterization of protozoan parasites," *Trends in parasitology*, vol. 21, no. 7, pp. 340–346, 2005.

[8] H. V. Smith and R. A. Nichols, "Cryptosporidium: detection in water and food," *Experimental parasitology*, vol. 124, no. 1, pp. 61–79, 2010.

[9] H. Bridle, *Waterborne Pathogens: Detection Methods and Applications*. Newnes, 2013.

[10] H. Bridle, B. Miller, and M. P. Y. Desmulliez, "Application of microfluidics in waterborne pathogen monitoring: A review," *water research*, vol. 55, pp. 256–271, 2014.

[11] J. Houssineau, "Representation and estimation of stochastic populations," Ph.D. dissertation, Heriot-Watt University, 2015.

[12] A. D. Goater, J. P. H. Burt, and R. Pethig, "A combined travelling wave dielectrophoresis and electrorotation device: applied to the concentration and viability determination of cryptosporidium," *Journal of Physics D-Applied Physics*, vol. 30, no. 18, p. L65, 1997.

[13] J. C. Mountford and M. Turner, "In vitro production of red blood cells," *Transfusion and Apheresis Science*, vol. 45, no. 1, pp. 85–89, 2011.

[14] H. Rhody, "Hough circle transform," *Chester F. Carlson Center for Imaging Science. Rochester Institute of Technology*, 2005.

[15] S. Kaur and M. Shukla, "Reversible data hiding in images using circular hough transform," *International Journal of Computer Science & Information Technologies*, vol. 5, no. 5, 2014.

[16] J. Houssineau, P. Del Moral, and D. E. Clark, "General multi-object filtering and association measure," in *Computational Advances in Multi-Sensor Adaptive Processing (CAMSAP), 5th IEEE Workshop on*, 2013.

[17] J. Houssineau, D. E. Clark, and P. Del Moral, "A sequential Monte Carlo approximation of the HISP filter," in *European Signal Processing Conference (EUSIPCO)*, 2015.

[18] Y. Pailhas, J. Houssineau, E. Delande, Y. Petillot, and D. E. Clark, "Tracking underwater objects using large MIMO sonar systems," in *International Conference on Underwater Acoustic*, 2014.

[19] D. Schuhmacher, B.-T. Vo, and B.-N. Vo, "A consistent metric for performance evaluation of multi-object filters," *Signal Processing, IEEE Transactions on*, vol. 56, no. 8, pp. 3447–3457, 2008.